Hindawi
International Journal of Photoenergy
Volume 2019, Article ID 9579357, 10 pages
https://doi.org/10.1155/2019/9579357

Research Article

Experimental Study on the Performance of a Phase Change Slurry-Based Heat Pipe Solar Photovoltaic/Thermal Cogeneration System

Hongbing Chen,[1] **Yutong Gong**,[1] **Ping Wei**,[2] **Pingjun Nie**,[1] **Yaxuan Xiong**,[1] **and Congcong Wang**[1]

[1]*School of Environment and Energy Engineering, Beijing University of Civil Engineering and Architecture, Beijing 100044, China*
[2]*School of Civil Engineering, Beijing Polytechnic Institute, Beijing 100038, China*

Correspondence should be addressed to Ping Wei; weipingbj@163.com

Received 9 October 2018; Revised 29 December 2018; Accepted 16 January 2019; Published 19 February 2019

Academic Editor: Huiqing Wen

By employing phase change slurry (PCS) as working fluid for the heat pipe solar PV/T system, the study is designed to investigate the electrical and thermal energy performance of the system. Meanwhile, through examining the performance difference between water-based and PCS-based heat pipe solar PV/T systems, 30% alkyl hydrocarbon PCS is proved to be a suitable working fluid for optimized energy performance based on the combined consideration of the thermophysical and rheological properties. Both static and dynamic stability tests show that 30% alkyl hydrocarbon PCS has a good stability for low-temperature thermal energy storage. A testing rig is constructed consisting of two identical heat pipe solar PV/T cogeneration systems A and B, in which water and 30% alkyl hydrocarbon PCS are, respectively, employed as working fluids; the energy performance of those two PV/T systems are investigated and compared with each other under the same testing condition. The results indicate that the application of PCS to the heat pipe PV/T system leads to a significant improvement in thermal performance and a modest growth in electrical performance. The daily heat gains and overall average efficiency of system B are 4.2 MJ/m^2 (per unit area of PV/T panel) and 59.3%, respectively, 27.3% and 9.3% higher than those of system A. Per unit area of the heat pipe PV/T panel could produce 55.2 L domestic hot water of about 45°C on a sunny day.

1. Introduction

In recent years, photovoltaic/thermal (PV/T) technology has been developed and put to use across the world [1]. Photovoltaic (PV) panel absorbs solar energy and converts part of them into electricity, and the rest of solar energy is stored in the PV panel as thermal energy. Then, the stored heat is transferred to working fluids by air/water type PV cooling [2], reducing PV cell working temperature and increasing PV electrical efficiency; at the same time, the heat absorbed from PV panel could be used for heating and/or domestic hot water supply. In examining the influence of different characters on PV/T collectors, several studies have revealed that the operating temperature of PV cells plays an important role in the performance of photovoltaic among these factors [3, 4]. Skoplaki and Palyvos [5] found that an increase in PV cell temperature would result in reduction of solar electrical efficiency. Therefore, in order to control the temperature of the cells, the accumulated heat need be removed from the back of the PV modules; the removed heat can also be reused. Many studies [6–10] have shown that although the water type PV/T system has better energy performance than the air type one, its cooling effect and energy performance are still moderate due to the limited heat transfer performance and water heat storage capacity. Therefore, a new idea, employing phase change slurry (PCS) as working fluid instead of water for PV/T system, is put forward [11]. In this case, the energy performance of PV/T system will be improved since both sensible and latent heat storage are produced, rather than only sensible heat storage, and more heat is absorbed from PV panel and transferred to PCS as well. On the other hand, the energy consumption of working fluid

circulation can be reduced based on the same heat storage load when the viscosity of PCS is significantly higher than that of water. The reason why under the same heat storage load PCS flow rate can be reduced in a much greater manner than water flow rate is that the heat storage capacities of per unit PCS and water are rather different.

Many studies have been carried out on PCSs and their combination with solar energy technology. Qiu et al. [12] investigated the energy performance of a novel microencapsulated phase change material (MPCM) slurry-based PV/T system under various solar radiations, slurry Reynolds numbers, and MPCM concentrations and concluded that the growth of Reynolds number and MPCM concentration of slurry contributes to the improvement of solar thermal efficiency and the decline of module temperature. By preparing phase change microemulsion and investigating its physical properties, Li et al. [13] revealed that the microemulsion had more latent heat and better stability. Studying the thermal efficiency and structural stability of paraffin microcapsule watery suspension (slurry A) and paraffin microemulsion (slurry B) before and after thermal cycling, Hadjieva et al. [14] concluded that slurry B produced better performance. By simulating a flat plate solar thermal collector with PCS as heat carrier by a numerical model, Serale et al. [15] demonstrated that the improvement in the instantaneous efficiency was in the range of 5% to 10%, while during the winter season the converted heat by the PCS-based system was 20~40% higher than that of a conventional water-based solar collector. The thermogravimetric analysis and thermal cycling tests of the 70% novel composite phase change material (PCM) were performed by Rao et al. [16], who indicated that 70% PCM had a good thermal stability and reliability. Building and testing three test rigs consisted of convectional PV panel, water-based photovoltaic/thermal system (PV/T) with double absorber plate, and water-based photovoltaic/thermal system with phase change material (PCM), Preet et al. [17] concluded that the maximum temperature reduction is 53% with water-based PV/T-PCM, and the electrical efficiency of water-based PV/T and water-based PV/T-PCM is higher than that of convectional PV panel. By comparing the overall energy efficiencies of the PV/T-PCM and PV/T systems, Yang et al. [18] found that the primary energy-saving efficiency for the PV/T-PCM system increased by 14%, which indicated that the energy performance of the PV/T system can be improved by combining PV/T with PCM. Diaconu [19] developed a theoretical model of the heat storage properties of PCSs capable of predicting the transient thermal response of a thermal energy storage system (TES). Aiming to develop microencapsulated PCSs that are stable enough to withstand the harsh conditions in the piping system, Gschwander et al. [20] built a test rig to perform thermal cycling of different PCSs, tested the stability of the microcapsules, and found that PCS based on microencapsulated paraffin has good stability. Conducting a heat storage experiment with fluid slurry composed of microencapsulated PCM, Zhang et al. [21] demonstrated that the PCM in the slurry has a strong effect on heat storage, which can shorten the heat storage time and lengthen the heat storage completion time due to the latent heat in the slurry. Yuan et al. [22] compared the performance of the PV/T systems with PCM to that of the PV/T systems with water and indicated that the electrical efficiency of the PV/T with PCM became higher than the electrical efficiency PV/T without PCM. By comparing a novel macroencapsulated phase change material- (PCM-) based solar photovoltaic thermal (PV/T) system and microchannel heat pipes (MCHP) PV/T system to a conventional PV/T system, Modjinou et al. [23] concluded that the combined daily average photothermal and electrical efficiency of encapsulated PCM is 36.71%, the highest, with MCHP and regular or conventional PV/T systems being 35.53% and 31.78%, respectively.

Some of the above studies mainly deal with PCS preparation and their properties, other studies are concerned with air/water-type or heat pipe-type PV/T systems, yet other studies investigate the energy performance of novel solar hot water systems combining PCM/PCS heat storage with solar collector. On the new PV/T systems with the combination of PCS heat storage with PV/T system and employing PCS as the working fluid of heat carrier, however, few studies have been carried out and reported. Compared with the conventional water-based heat pipe PV/T system, the new system employs PCS as heat carrier, and the heat transfer performance between the condensation section of heat pipes and heat carrier in the manifold will be enhanced in that the water temperature increases during the heat transfer process in the manifold while the PCS temperature almost remains constant due to the occurrence of phase change. Therefore, the temperature difference between the condensation section of heat pipes and heat carrier (water and PCS) would lead to different heat transfer performance.

The purposes of this study are twofold: one is to employ PCS as working fluid for the heat pipe solar PV/T system and investigate the electrical and thermal energy performance of the system and the other is to identify any performance improvement of the PCS-based heat pipe solar PV/T system, in comparison with the conventional water-based one under the same working condition.

2. Description of the Heat Pipe PV/T System

The testing rig consists of two identical heat pipe solar PV/T cogeneration systems, where the water and 30% alkyl hydrocarbon PCS are employed as working fluids, respectively, in systems A (water based) and B (PCS based). Presented in Figure 1 is the picture of the testing rig. The experimental set-up of the heat pipe solar PV/T cogeneration system, including heat pipe PV/T collector, heat exchange water tank, expansion tank, circulating pump, flow meter and power test circuit. The heat pipe PV/T collector is mainly made up of PV panel, heat pipes, aluminium sheet, manifold, and insulation layer. The PV panel has a nominal power of 305 W with a size of 1950 mm × 982 mm, and its backboard is composed of white Tedlar-polyester-Tedlar (TPT) with a PV packing factor of 0.95. The evaporation section of heat pipes is adhered onto the back surface of PV panel with thermal silica gel for good thermal conductance. To reduce the thermal contact resistance between heat pipes and PV panel and enhance heat transfer performance, the heat pipes are

Figure 1: The testing rig of two identical heat pipe solar PV/T cogeneration systems A and B.

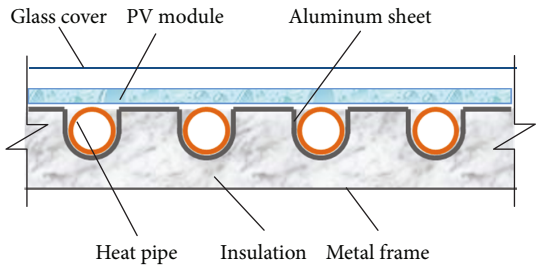

Figure 2: Cross-sectional view of heat pipe PV/T panel.

tightly partial-wrapped with thin aluminium sheet at the evaporation sections under precise pressure control to ensure a good contact between heat pipes and aluminium sheet, and the thin aluminium sheet is also pasted onto the back surface of PV panel with thermal silica gel. The condensation sections of heat pipes are inserted into the manifold with a heat pipe pitch of 75 mm. In addition, a glass covering and a sponge rubber insulation layer (50 mm in thickness) are installed at the front and back surfaces of PV panel for preventing dust particles and heat loss, respectively. The cross-sectional view of heat pipe PV/T panel is shown in Figure 2.

The diagram of the PCS-based heat pipe solar PV/T cogeneration system is shown in Figure 3. When solar light irradiates on the PV panel, part of the solar energy is converted into electricity and the rest is converted into thermal energy. The thermal energy stored in PV panel, flowing across the backboard of PV panel and the aluminium sheet, is transferred to the evaporation section of heat pipes. The working medium in heat pipes absorbs heat and evaporates at the evaporation section and changes to vapor phase accordingly. Then, the working medium vapor moves from the evaporation section to the condensation section due to low density and releases heat at the condensation section of heat pipes, where it turns into liquid again and flows back to the evaporation section to finish the cycle as a result of gravity effect.

When the PCS flows through the manifold, the PCS absorbs heat from the conservation section of heat pipes, which are inserted into the manifold. As the temperature of PCS rises up to the phase change initial temperature, the PCM particles of PCS start to change from solid phase to liquid phase with heat charging in PCS. Then, the PCS is circulated to the heat exchange water tank, where it releases heat to cold water and the PCM particles change from liquid phase to solid phase with heat discharging from PCS. Therefore, the cold water in heat exchange tank is heated step by step, and the thermal energy is transferred from PV panel to cold water by the above circulation in the end.

Figure 3 presents the contents and locations of the test points, including solar radiation (G), outdoor air temperature (T1), inlet and outlet water temperature (T2, T3) of the manifold, water temperature (T4) in heat exchanger water tank and surface temperature (T5, T6, T7, and T8) of photovoltaic panels, and the volumetric flowrate (m) of working fluid flowing through the manifold. To ensure the accuracy of the measured surface temperature of photovoltaic panels, the four corners of the photovoltaic panel have been selected as the four testing points. The inlet and outlet temperature of the manifold, the outdoor air temperature, and the water temperature in the heat exchange water tank are all measured by platinum resistance temperature sensor, while the surface temperature of the photovoltaic panel is measured by type K adhesive thermocouple temperature sensor. Meanwhile, an inverter is connected to PV panel for the converting of direct current (DC) to alternating current (AC). Two current and voltage sensors are installed at the circuit between the PV panel and the inverter to measure the electrical power output. The testing devices for the system performance are shown in Table 1.

3. Performance Assessment and Experiment Implementation

3.1. Performance Assessment. The instantaneous electrical power output can be calculated by

$$q_{ele} = UI, \tag{1}$$

where U is the voltage measured by voltage sensor and I is the current measured by current sensor.

The electrical efficiency can be calculated by

$$\eta_{ele} = \frac{q_{ele}}{GA_c\zeta}, \tag{2}$$

where G is the solar radiation intensity, A_c is the collector area, and ζ is the PV packing factor which is valued 0.95 in this paper.

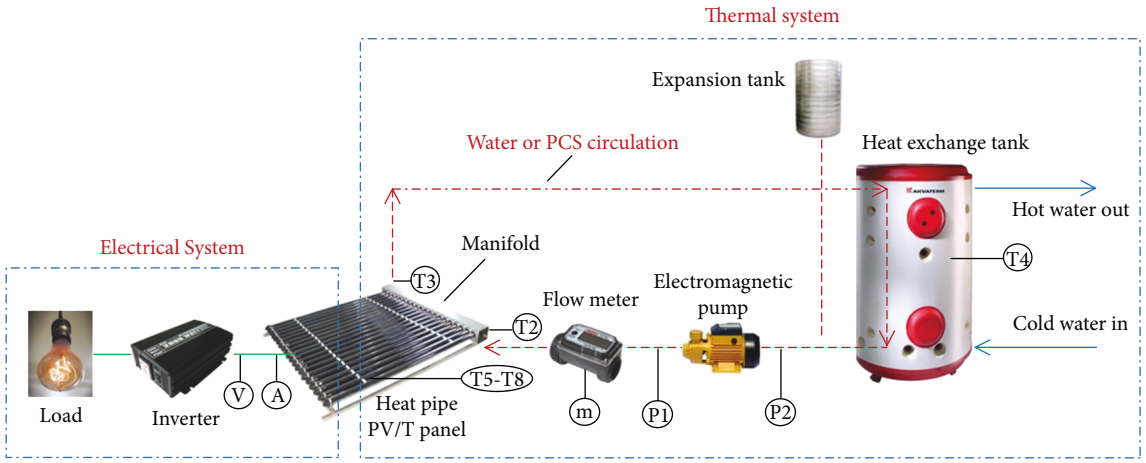

Figure 3: Diagram of heat pipe solar PV/T cogeneration system.

Table 1: List of testing devices.

Item	Device	Quantity	Testing inaccuracy
1	Pyranometer (TBQ-2-B)	1	±2.0%
2	Platinum resistance temperature sensor (WZP-01)	7	±0.5%
3	Adhesive thermocouple type K (WZPM-02)	8	±0.5%
4	Electromagnetic flow meter (SE115MM)	2	±0.5%
5	Current sensor (WBI022F21)	2	±1.0%
6	Voltage sensor (WBV342UO1-S)	2	±0.2%
7	Pressure transducer (YB-131)	4	±0.5%
8	Data logger (Agilent 34972A)	1	

The instantaneous thermal power output of the PV/T panel of system A can be calculated by

$$q_{\text{th}} = c_w \rho_w v_w (T_{\text{out}} - T_{\text{in}}), \tag{3}$$

where c_w is the specific heat capacity of water, ρ_w is the density of water, v_w is the circulating volume flow of system A, and T_{in} and T_{out} are the inlet and outlet temperatures of the manifold.

For system B (PCS based), the calculation of the instantaneous thermal power output of the PV/T panel is different before, during, and after the phase change process, respectively.

The instantaneous thermal power output of the PV/T panel of system B before the phase change can be calculated by

$$q_{\text{th}} = c_{s,\text{before}} \rho_s v_s (T_{\text{out}} - T_{\text{in}}), \tag{4}$$

where $c_{s,\text{before}}$ is the specific heat capacity of PCS before phase change, ρ_s is the density of PCS, and v_s is the circulating volume flow of system B.

The instantaneous thermal power output of the PV/T panel of system B during the phase change progress can be calculated by

$$q_{\text{th}} = \rho_s v_s r, \tag{5}$$

where r is the latent heat of phase change.

The instantaneous thermal power output of the PV/T panel of system B after the phase change can be calculated by

$$q_{\text{th}} = c_{s,\text{after}} \rho_s v_s (T_{\text{out}} - T_{\text{in}}), \tag{6}$$

where $c_{s,\text{after}}$ is the specific heat capacity of PCS after the phase change.

The combined daily average thermal efficiency can be calculated by

$$\overline{\eta}_{th} = \frac{\sum_{i=1}^{n} q_{th,i}}{A_c \sum_{i=1}^{n} G_i}. \tag{7}$$

The combined daily average overall efficiency [24] can be calculated by

$$\overline{\eta}_{\text{ov}} = \overline{\eta}_{\text{th}} + \zeta \frac{\overline{\eta}_{\text{ele}}}{\eta_{\text{power}}}, \tag{8}$$

where η_{power} is the power generation efficiency of the conventional thermal power plants which in this paper values 0.38.

3.2. Experiment Implementation. The experimental rig is established on the roof of a building in Beijing University of Civil Engineering and Architecture located at north of China (116.3 E, 39.9 N). The PV panels are installed to be south facing with a tilt angle of 30°. The circulating water flow rates of systems A and B are both set to be 6 L/min, and the volume of heat exchange tank for each system is 100 L. The testing lasts for 8 hours every day from 8:30 am to 16:30 pm with a data collection interval of 2 min, and the test is carried out in May and June 2016.

Table 2: Physical properties of PCS.

Concentration (%)	Phase change temperature (°C)	Specific heat capacity (kJ/kg·°C)	Density (kg/m^3)	Latent heat (kJ/kg)	Viscosity (mPa·s)
30	35	2.95	900	50.3	23.2
—	41	3.2	880	—	20.7

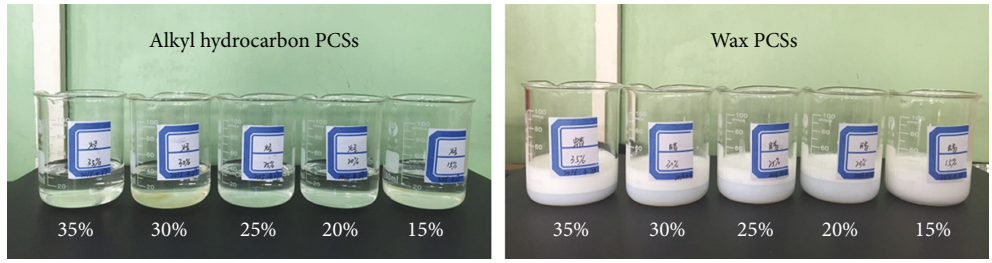

Figure 4: The picture of alkyl hydrocarbon PCS and wax PCS after ten months' steady placement.

Apart from the electrical power output, the heat pipe PV/T system is operating for the low-temperature heat collection and domestic hot water supply. Therefore, some kinds of commonly used and cheap commercialized phase change material with the phase change temperature of around 40°C will be suitable for the study. In our previous study [25], two types of alkyl hydrocarbon and wax phase change slurries (PCSs) were chosen for the property comparison after the literature review. The alkyl hydrocarbon PCS and wax PCS with different mass concentrations of 15%, 20%, 25%, 30%, and 35% were, respectively, prepared for low-temperature thermal energy storage, and the thermophysical and rheological properties of those PCSs were tested and compared with each other. The results indicated that the 30% alkyl hydrocarbon PCS was the most suitable one for optimized energy performance in solar heat collection based on its thermophysical and rheological properties. Consequently, the 30% alkyl hydrocarbon PCS is selected for stability test and further study in the paper. The detailed physical properties of the 30% alkyl hydrocarbon PCS are shown in Table 2.

The stability test is carried out in static and dynamic modes. Two tasks are involved in the static stability test: one is to check whether there is any occurrence of sediment and stratification of PCS after several months' static replacement and the other is to check whether there are any changes of the thermophysical and rheological properties of PCS after several months' static replacement. The differential scanning calorimeter (DSC) is used for the testing of the thermophysical property, and the digital viscometer is used for the testing of the rheological property. For the detailed information of DSC and digital viscometer as well as the testing process, a reference to our previous study [25] is recommended. The dynamic stability test is presented by the performance comparison of the thermophysical property of PCS after dozens of times of thermal cycles (i.e., heat charge and discharge cycles).

All those abovementioned alkyl hydrocarbon and wax PCSs are placed in static state at room temperature for ten months. Presented in Figure 4 is the picture of alkyl hydrocarbon and wax PCSs after ten months' steady placement. It can be seen from Figure 4 that the occurrence of sediment and stratification is found in the wax PCS while not in the alkyl hydrocarbon PCS, which indicates that the alkyl hydrocarbon PCS has a better stability.

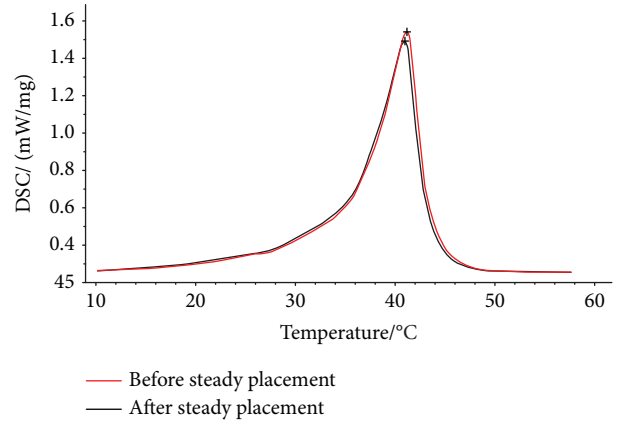

Figure 5: DSC curves of the 30% alkyl hydrocarbon PCS before and after ten months' steady placement.

As indicated in Figure 5 the two DSC curves of PCS before and after long time steady placement are almost the same. The initial phase change temperature and peak temperature are about 35.0°C and 41.2°C, and the phase change latent heat is about 50.3 J/g. The testing results reveal that the 30% alkyl hydrocarbon PCS has a stable thermophysical property in the steady state over a period of time of ten months.

As illustrated in Figure 6, the viscosity of the 30% alkyl hydrocarbon PCS increases by 5.39~14.78% after ten months' steady placement, which is caused by the volatilization of water vapor. By increasing the air tightness of the container and correspondingly reducing the volatilization of water vapor, the viscosity stability of the 30% alkyl hydrocarbon PCS could be further improved.

As shown in Figure 7, the maximum phase change temperature is 35.5°C and the minimum value is 34.6°C with a

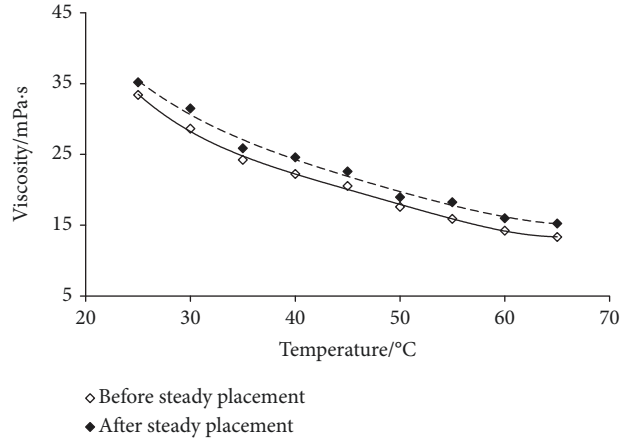

Figure 6: Viscosity of 30% alkyl hydrocarbon PCS before and after ten months' steady placement.

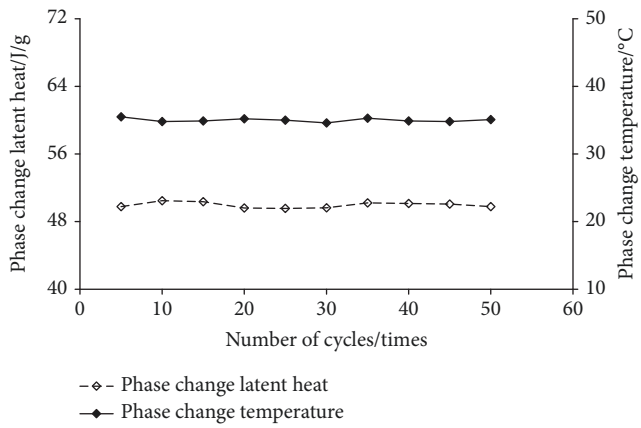

Figure 7: Phase change temperature and phase change latent heat of the 30% alkyl hydrocarbon PCS before and after multiple thermal cycles.

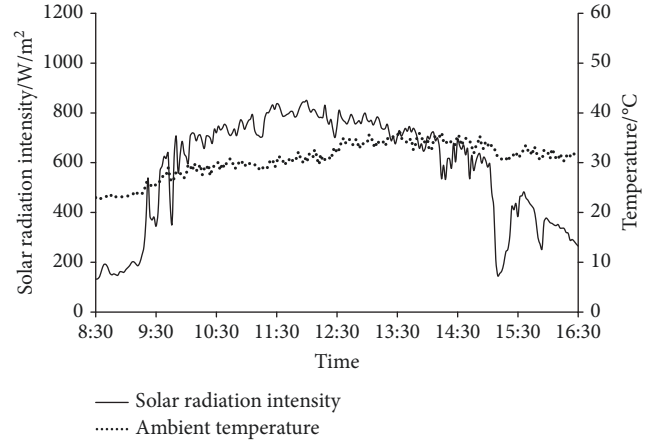

Figure 8: Solar radiation and ambient temperature.

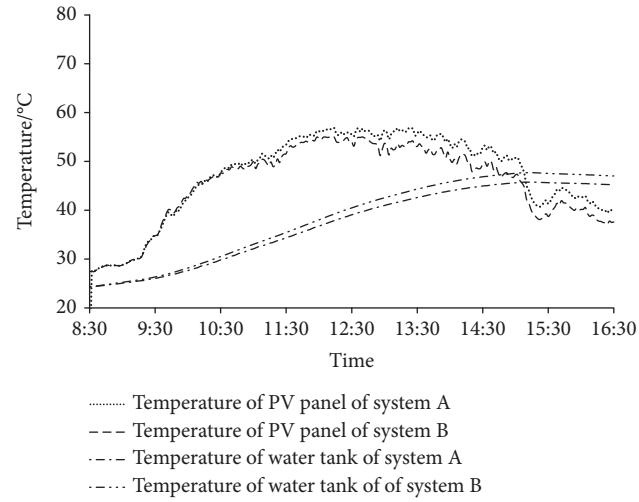

Figure 9: Temperature variation of PV panel and water of heat exchange tank.

difference of 2.54%. The maximum phase change latent heat is 50.48 J/g and the minimum value is 49.56 J/g with a difference of 1.82%. The phase change temperature and phase change latent heat are almost constant over multiple thermal cycles, which indicates that the thermophysical property of the 30% alkyl hydrocarbon PCS still maintain a steady state after dozens of times of thermal cycles.

The above stability test indicates that the 30% alkyl hydrocarbon PCS has a quite good stability and it can act as a suitable working fluid for low-temperature thermal energy storage in solar PV/T cogeneration system.

4. Results and Discussion

4.1. Solar Radiation and Ambient Temperature. Figure 8 shows the solar radiation and ambient temperature on a testing day. The mean solar radiation is 581.7 W/m^2 and the mean ambient temperature is 30.7°C. As illustrated in Figure 8, the solar radiation increases before 12:00 pm and reaches the maximum value of 849.7 W/m^2 at about 12:00 pm. After that, it decreases gradually. There is a sharp decrease of solar radiation from 623 W/m^2 to 156 W/m^{2}at 15:00 pm, which is mainly caused by cloud shading.

4.2. Temperature Variation of PV Panel and Water of Heat Exchange Tank. As shown in Figure 9, the PV panel temperature increases in the morning, reaching the maximum at noon time, and decreases in the afternoon, which suggests a similar changing trend with the solar radiation. The PV panel temperatures of systems A (water based) and B (PCS based) are almost the same before 11:00 am, and after that, the PV panel temperature of system A is notably higher than that of system B, which suggests that more heat is extracted from the PV panel of system B. As the working fluid (water or PCS) absorbs heat in the manifold, its temperature increases as a result. The water temperature increases all the time during the heat transfer process. The PCS temperature increases before it reaches the phase change initial temperature at about 11:00 am, which is similar to the changes of water temperature; afterwards, during the phase change process, the PCS temperature almost remains constant. Therefore, the temperature difference between the condensation section of

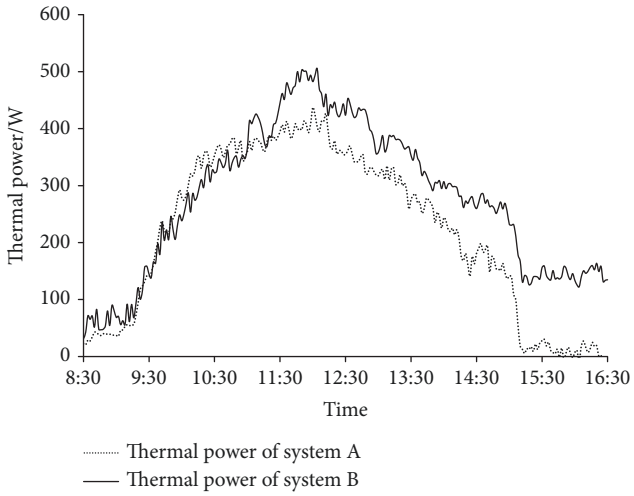

Figure 10: Variation of the thermal power.

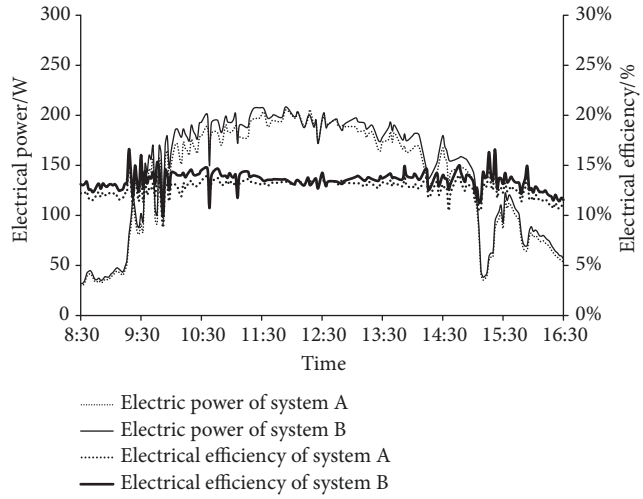

Figure 11: Variation of electrical power and electrical efficiency.

heat pipes and the PCS would be higher, which leads to more heat transferred to PCS and the PV panel temperature of system B would be lower accordingly.

It can also be seen from Figure 9 that the water temperature of heat exchange tank increases with the time and almost remains stable after it reaches a certain value. The water temperatures of systems A and B exhibit a similar changing trend. The cold water of systems A and B are, respectively, heated from 25°C to 45°C and 47°C. The heat storage caused by phase change of PCS in system B leads to more heat collection of system B than that of system A. However, due to the low thermal conductivity of PCS and the limited time for heat transfer in the manifold and heat exchange tank during each working fluid circulation, the heat charging and discharging process of PCS might be insufficient, which means the thermal performance could be further improved if many kinds of nanoparticles are added to enhance the heat conductivity of PCS and/or the optimization of system operation is conducted.

4.3. Thermal Power and Thermal Efficiency. As can be seen in Figure 10, the thermal power grows gradually before 12:00 pm, reaching the maximum at about 12:00 pm, and then it decreases in the afternoon. The thermal power of system A is slightly higher than that of system B before 11:00 am. The reason for the slight difference between the thermal power of systems A and B can be explained as follows. Before the PCS reaching its phase changes initial temperature, the heat transfer process between the working fluid (water or PCS) and the condensation section of heat pipes only involves sensible heat transfer when it flows through the manifold. However, the specific heat capacity of PCS is lower than that of water, leading to slight lower thermal power of system B. As the PCS reaches the phase change initial temperature after 11:00 am, it starts to absorb a great amount of phase change latent heat, leading to a sharp increase of thermal power of system B, about 100 W higher than that of system A. With the rise of working fluid temperature, the temperature difference between the condensation section of heat pipes and working fluid decreases as a result, leading to the decline of thermal power as well. After about 15:10 pm, the temperature difference of system A tends to be zero, and accordingly, there is almost no thermal power output.

The maximum thermal powers and daily average thermal powers of systems A and B are, respectively, 436.9 W *vs.* 505.4 W and 219.7 W *vs.* 276.7 W. The daily heat gains of system B is 4.2 MJ/m^2 (per unit area of PV/T panel), 27.3% higher than 3.3 MJ/m^2, that of system A.

In consideration of thermal inertia, the thermal efficiencies of system A and B are evaluated as the combined daily average values. It is calculated that the combined daily average thermal efficiency of systems A and B are 19.3% and 24.3%, respectively.

4.4. Electrical Power and Electrical Efficiency. As illustrated in Figure 11, the electrical power curves of both systems are consistent with each other with a slight difference, which show the similar changing trend of solar radiation. The daily average electrical powers of systems A and B are, respectively, 125.6 W and 133.7 W, with a difference of 6.4%. The electrical efficiency fluctuates slightly during the testing, and the electrical efficiency of system B is slightly higher than that of system A. The average daily electrical efficiencies of systems A and B are, respectively, 13.2% and 14.0%. It is well known that the PV electrical efficiency rises with the PV working temperature's decline. The relationship between the PV electrical efficiency and PV working temperature has been investigated by many researchers and the results have been published and presented with known formulas. As shown in Section 4.2, the PV panel temperature of system B is lower than that of system A in that more heat is absorbed from PV panel as a result of the PCS latent heat charging. Therefore, the modest increase obtained in the electrical efficiency of system B is attributed to the decrease of PV working temperature, which is also consistent with previous findings.

4.5. Efficiency Comparison. Figure 12 shows the comparison of daily average thermal, electrical, and total efficiencies

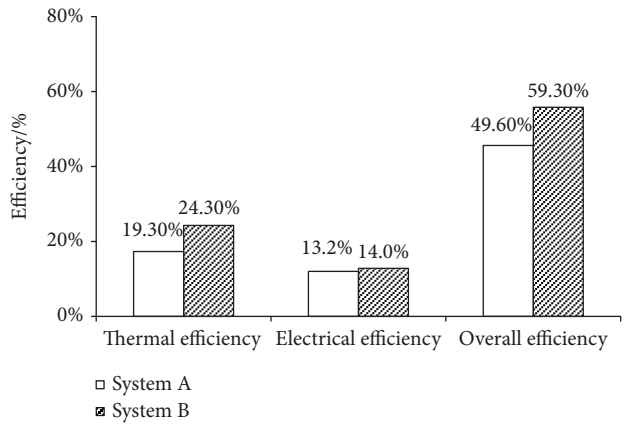

Figure 12: Comparison of daily average efficiency.

between two systems. It can be seen from Figure 12 that the daily average thermal efficiency of system B is 5% higher than that of system A and the daily average electrical efficiency is 0.8% higher as well, leading to 9.7% higher of the daily average overall efficiency of system B. The thermal efficiency is not as high as expected and it can be improved by adding more heat pipes under PV panel and replacing the white TPT PV backboard with a dark one of higher absorbance and higher heat conductivity, and the heat gain of PV panel will increase as well, which leads to better thermal performance. In addition, reducing PV packing factor can also increase the heat gains of PV panel and further improve thermal performance as well. However, the electrical power output will be reduced due to less PV area in that case while there will be little impact on electrical efficiency.

Regarding the confidence limits of the results, it is true that the inaccuracies of testing devices will certainly affect the testing results. The errors caused by the inaccuracies of testing devices are called systematic errors, which are inevitable but can be reduced by using testing devices with improved accuracy. Since the systematic errors of the testing results generally present the directional and repeated deviation and the same testing devices are used for the testing of both systems A and B, the systematic errors of the testing results of system A will be consistent with that of system B. Meanwhile, this study is mainly aimed to investigate the performance difference between the PCS-based and water-based PV-T systems and to identify the performance improvement as well. Therefore, the systematic errors of the testing results should have little impact on the performance difference, and the effect of the systematic errors on the main results could be negligible.

4.6. Economic Analysis. In our previous study [26] concerning the application of the water-based heat pipe PV-T system to a house in the rural area of the northern China, the simple payback time is about 14.2 years. In this study, the working fluid (water) is replaced with PCS and the initial investment increases by about 6% (300 RMB), while the energy performance improvement increases by about 9.7%. Therefore, the simple payback time will be around 13.7 years. The simple payback time tends to vary in different areas.

5. Conclusions

To study on the performance of a PCS-based heat pipe solar PV/T cogeneration system, in the current study, a testing rig is constructed, which consists of two identical heat pipe solar PV/T cogeneration systems, namely, system A and system B. With water as working fluids in system A and 30% alkyl hydrocarbon PCS in system B, the energy performance of the two PV/T systems are investigated and compared with each other under the same working condition. The conclusions are as follows:

(1) Through the test and comparison of the thermophysical and rheological properties of the alkyl hydrocarbon and wax PCSs, the 30% alkyl hydrocarbon PCS is proved to be the most suitable one for optimized energy performance. The static and dynamic stability tests indicate that the 30% alkyl hydrocarbon PCS also has a quite good stability

(2) Compared with the water-based heat pipe PV/T system, the application of PCS to the heat pipe PV/T system leads to a significant improvement in thermal performance while a modest improvement in electrical performance

(3) The daily average overall efficiency of system B (PCS based) is 59.3%, 9.7% higher than that of system A (water based). The daily heat gains of system B (PCS based) are 4.2 MJ/m^2 (per unit area of PV/T panel), 27.3% higher than that of system A (water based)

(4) Per unit area of the heat pipe PV/T panel could produce 55.2 L domestic hot water of about 45°C on a sunny day. The thermal performance could be improved by replacing the white TPT PV backboard with a dark one of higher absorbance and higher heat conductivity and/or reducing PV packing factor

Parameters

A: Area, m^2
c: Specific heat capacity, J/(kg·K)
G: Solar radiation intensity, W/m^2
I: Electrical current, A
q: Power, W
r: Latent heat of phase change, J/kg
T: Temperature, K
U: Voltage, V
v: Circulating volumetric flowrate, m^3/s.

Greek Letters

η: Efficiency
ζ: PV packing factor
ρ: Density, kg/m^3.

Subscripts

a: Ambient

after: After the phase change
before: Before the phase change
c: Collector
ele: Electrical
in: Inlet
out: Outlet
ov: Overall
s: PCS
th: Thermal
w: Water.

Data Availability

The data used to support the findings of this study are available from the corresponding author upon request.

Conflicts of Interest

The authors declare that they have no conflicts of interest.

Acknowledgments

The work of this paper is fully supported by Projects of National Key Research and Development Program (2016YFE0102300–08, 2016YFC0700104) and Beijing Advanced Innovation Center for Future Urban Design (UDC2016040200).

References

[1] A. K. Pandey, V. V. Tyagi, J. A./. L. Selvaraj, N. A. Rahim, and S. K. Tyagi, "Recent advances in solar photovoltaic systems for emerging trends and advanced applications," *Renewable & Sustainable Energy Reviews*, vol. 53, pp. 859–884, 2016.

[2] X. Zhang, X. Zhao, S. Smith, J. Xu, and X. Yu, "Review of R&D progress and practical application of the solar photovoltaic/thermal (PV/T) technologies," *Renewable & Sustainable Energy Reviews*, vol. 16, no. 1, pp. 599–617, 2012.

[3] R. Liang, J. Zhang, L. Ma, and Y. Li, "Performance evaluation of new type hybrid photovoltaic/thermal solar collector by experimental study," *Applied Thermal Engineering*, vol. 75, pp. 487–492, 2015.

[4] J. Zhang, Y. Xuan, and L. Yang, "Corrigendum to "Performance estimation of photovoltaic–thermoelectric hybrid systems" [Energy 78 (2014) 895–903]," *Energy*, vol. 81, pp. 804-805, 2015.

[5] E. Skoplaki and J. A. Palyvos, "On the temperature dependence of photovoltaic module electrical performance: a review of efficiency/power correlations," *Solar Energy*, vol. 83, no. 5, pp. 614–624, 2009.

[6] J. Prakash, "Transient analysis of a photovoltaic-thermal solar collector for co-generation of electricity and hot air/water," *Energy Conversion and Management*, vol. 35, no. 11, pp. 967–972, 1994.

[7] S. Y. Wu, C. Chen, and L. Xiao, "Heat transfer characteristics and performance evaluation of water-cooled PV/T system with cooling channel above PV panel," *Renewable Energy*, vol. 125, pp. 936–946, 2018.

[8] L. Q. Tang, Q. Z. Zhu, S. C. Jing, M. Y. Wu, and J. W. Lu, "Performance study of flowing-over water cooled PV/T system," *Acta Energiae Solaris Sinica*, vol. 36, pp. 860–864, 2015.

[9] B. Hu, S. Y. Yan, and H. Z. Zhang, "Study on heat transfer performance of water-cooled PV/T collector," *Renewable Energy Resources*, vol. 2, pp. 164–170, 2015.

[10] Q. Z. Zhu, L. Q. Tang, J. D. Li, C. Li, and H. Chen, "Experimental study of water-cooled panel type PV/T system in winter," *Journal of Thermal Science and Technology*, vol. 4, pp. 316–320, 2014.

[11] G. Serale, Y. Cascone, A. Capozzoli, E. Fabrizio, and M. Perino, "Potentialities of a low temperature solar heating system based on slurry phase change materials (PCS)," *Energy Procedia*, vol. 62, pp. 355–363, 2014.

[12] Z. Qiu, X. Ma, X. Zhao, P. Li, and S. Ali, "Experimental investigation of the energy performance of a novel microencapsulated phase change material (MPCM) slurry based PV/T system," *Applied Energy*, vol. 165, pp. 260–271, 2016.

[13] Y. K. Li, S. D. Ma, and G. Y. Tang, "Research on physical properties and stability of phase change microemulsion," *Journal of Functional Materials*, vol. 41, no. 10, pp. 1813–1815, 2010.

[14] M. M. Hadjieva, M. Bozukov, and I. Gutzov, "Next generation phase change materials as multifunctional watery suspension for heat transport and heat storage," *MRS Proceedings*, vol. 1188, 2009.

[15] G. Serale, S. Baronetto, F. Goia, and M. Perino, "Characterization and energy performance of a slurry PCM-based solar thermal collector: a numerical analysis," *Energy Procedia*, vol. 48, pp. 223–232, 2014.

[16] Z. Rao, T. Xu, C. Liu, Z. Zheng, L. Liang, and K. Hong, "Experimental study on thermal properties and thermal performance of eutectic hydrated salts/expanded perlite form-stable phase change materials for passive solar energy utilization," *Solar Energy Materials and Solar Cells*, vol. 188, pp. 6–17, 2018.

[17] S. Preet, B. Bhushan, and T. Mahajan, "Experimental investigation of water based photovoltaic/thermal (PV/T) system with and without phase change material (PCM)," *Solar Energy*, vol. 155, pp. 1104–1120, 2017.

[18] X. Yang, L. Sun, Y. Yuan, X. Zhao, and X. Cao, "Experimental investigation on performance comparison of PV/T-PCM system and PV/T system," *Renewable Energy*, vol. 119, pp. 152–159, 2018.

[19] B. M. Diaconu, "Transient thermal response of a PCS heat storage system," *Energy and Buildings*, vol. 41, no. 2, pp. 212–219, 2009.

[20] S. Gschwander, P. Schossig, and H. Henning, "Micro-encapsulated paraffin in phase-change slurries," *Solar Energy Materials and Solar Cells*, vol. 89, no. 2-3, pp. 307–315, 2005.

[21] Y. Zhang, S. Wang, Z. Rao, and J. Xie, "Experiment on heat storage characteristic of microencapsulated phase change material slurry," *Solar Energy Materials & Solar Cells*, vol. 95, no. 10, pp. 2726–2733, 2011.

[22] W. Yuan, J. Ji, M. Modjinou et al., "Numerical simulation and experimental validation of the solar photovoltaic/thermal system with phase change material," *Applied Energy*, vol. 232, pp. 715–727, 2018.

[23] M. Modjinou, J. Ji, W. Yuan et al., "Performance comparison of encapsulated PCM PV/T, microchannel heat pipe PV/T and conventional PV/T systems," *Energy*, vol. 166, pp. 1249–1266, 2019.

[24] B. J. Huang, T. H. Lin, W. C. Hung, and F. S. Sun, "Performance evaluation of solar photovoltaic/thermal systems," *Solar Energy*, vol. 70, no. 5, pp. 443–448, 2001.

[25] C. Hongbing, C. Sai, Z. Lei, L. Danming, and L. Qiang, "Selection and property study of phase change slurry for solar heat collection," *Energy Procedia*, vol. 105, pp. 4059–4064, 2017.

[26] Q. Wang, *Study on the performance of PV/heat pipe heat pump system*, Beijing University of Civil Engineering and Architecture, Beijing, China, 2015.